Continuum Force Microscopy Study of the Elastic Modulus, Hardness and Friction of Polyethylene and Polypropylene Surfaces

D. H. Gracias and G. A. Somorjai*

Department of Chemistry, University of California at Berkeley, Berkeley, California 94720, and Materials Science Division, Lawrence Berkeley National Laboratory, Berkeley, California 94720

Received May 15, 1997; Revised Manuscript Received October 22, 1997

ABSTRACT: The atomic force microscope (AFM) has been modified to a continuum force microscope (CFM) by using a tip of a large radius of curvature (1000 nm), in an attempt to reduce the pressure in the contact region. The elastic modulus, hardness, and friction of the surfaces of low density polyethylene, high density polyethylene, isotactic polypropylene, and atactic polypropylene have been quantitatively measured at low loads (10^{-8}−10^{-6} N) with the CFM. The effect of pressure applied by the tip has been observed in the measurements, resulting in an increase in the elastic modulus and the shear strength of the polymer surface with increasing pressure. The effect of pressure increases with decreasing density of the polymer. The higher values of elastic modulus and hardness of the polymer surface correlate well with the higher crystallinity of the polymers. Frictional properties of the polymers show characteristics that can be explained by the JKR model; the relative frictional behavior of the polyolefin surfaces however is controlled by the deformation component of the friction, i.e., the yield strength, the elastic modulus and the pressure dependence of the shear strength.

Introduction

Understanding the mechanical properties (elastic modulus, hardness, and friction) of polymers at the surface and near surface region is crucial to many of their applications. These properties can be measured only at low loads, which can be carried out with the atomic force microscope (AFM),[1] which also provides a nanoscale level scrutiny of the polymer surface. At higher loads, the probes that monitor polymer mechanical properties break through the surface layer, and therefore measure bulk values on the macroscopic scale and some excellent books are available on the subject.[2−6] The AFM has been used successfully to measure elastic modulus, hardness and friction on many systems.[7−11] However the pressure applied by the typical silicon nitride AFM tip (tip radius of 20−50 nm), used in these experiments, is extremely high, even at very small loads.

Figure 1 shows a theoretical plot of the mean pressure P, at the contact between a single asperity of radius R, and a planar surface vs the load (W) applied as predicted by Hertzian contact mechanics,[12] defined by the expression

$$P = \frac{2}{3}\left(\frac{6WE^{*2}}{\pi^3 R^2}\right)^{1/3} \qquad (1)$$

As can be seen from the figure, the contact pressure depends more strongly on the radius of the tip than on the load. For example, the pressure applied by a tip of radius 20 nm (typical radius of commercial ultralevers used in AFM) at 1 nN is equal to the pressure applied by a tip of radius 1000 nm at a load of 2.5 μN.

While working on soft materials such as polymers it is important to keep the pressure in the contact region low, to do meaningful experiments without considerable deformation of the polymer surface. To reduce the pressure at the contact, we must use blunt tips, thereby sacrificing spatial resolution but keeping the pressure low. In the present study we have used a tip with a large radius of curvature (1000 nm). The mean pressures being applied are considerably lower than similar experiments done with the AFM till date.[7−11] By using a tip of a large radius, however, we are now measuring continuum and not atomic forces, and this justifies the term "continuum force microscopy" (CFM).

In this study, we have used a CFM to monitor the elastic modulus, hardness, and friction of a series of polyolefins, i.e., low and high-density polyethylene (LDPE and HDPE) and isotactic and atactic polypropylene (IPP and APP) in the load range of 10^{-8}−10^{-6} N. The reason for studying the above polymers, is that

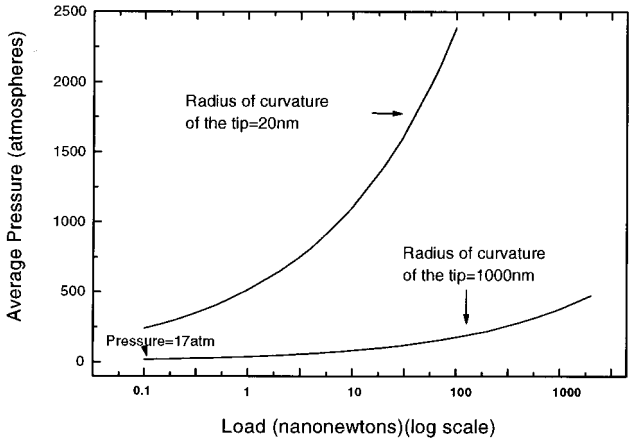

Figure 1. A theoretical plot of the average pressure (P) applied by tip (as given by the Hertzian model of continuum mechanics) vs load (W) i.e., eq 1, for two tips of radii of curvature 20 and 1000 nm. The pressure is calculated for a junction of modified elastic modulus of 1 GPa, which is a typical value for the polymers examined. The pressure under the tip is extremely high even at small loads and depends strongly on the radius of curvature of the tip. To reduce the effect of high pressure under the tip we have used a tip of radius 1000 nm in the continuum force microscope as opposed to a tip of radius 20 nm used typically in ultralevers in atomic force microscopy.

* To whom all correspondence should be addressed at the University of California.

S0024-9297(97)00683-9 CCC: $15.00
Published on Web 01/28/1998

they provide fundamental systems for studying the effect of density, tacticity, and crystallinity on the mechanical properties of polymer surfaces composed of similar hydrophobic monomer units. Moreover we would like to address crucial phenomenon like the low friction coefficient observed on high-density polyethylene.[13]

To do a systematic study of the surface mechanical properties, thereby justifying a comparison of the relative mechanical properties based on the intrinsic properties of the polymer, we have reduced the number of variables affecting the measurements. The polymers were processed in the same manner and characterized extensively. Special care was taken to prepare smooth surfaces; the mechanical measurements were done on all the polymers using the same well-calibrated experimental set up, i.e., with the same tip, with the same environment, and at the same velocity/frequency.

To our knowledge this is the first quantitative measurement of the elastic modulus, hardness, and friction of polyethylene and polypropylene in this load regime We have measured the radius of the tip accurately and have applied continuum contact mechanics to explain the experimental results.

We have demonstrated the effects of high pressure in our measurements. The elastic modulus is found to increase with increasing pressure. Friction vs load curves show characteristics predicted by the JKR model[14] such as friction at negative loads, i.e., when the tip and surface are in the attractive regime, and pull-off forces (a finite force required to separate the bodies in contact); however, a dependence of the shear strength on pressure is observed for LDPE and IPP, which results in a linear dependence of frictional force and load.

The expected trend of increasing elastic modulus and hardness with increasing density and crystallinity was observed. The friction process in all cases is dominated by the deformation of the polymer surface. Even though the surface energy, elastic modulus, and hardness of HDPE as compared to those of IPP are similar, the friction coefficient measured on HDPE is much lower than that of IPP. This has been attributed to a negligible increase in the shear strength of HDPE with increasing pressure, due to the high density of the polymer.

Experiments

Sample preparation and characterization. LDPE, HDPE, IPP, and APP were purchased from Aldrich in the form of pellets. The polymers were melted on a Pyrex glass plate in air while pressing on them with a weight of around 10 kg for an hour. The polymer was cooled by taking it off the hot plate. The polymer cools to room temperature in around 20 min. The polymer was then peeled off. The surface of the polymer in contact with the glass plate was used to measure the various mechanical properties mentioned above. This method of preparation was used as it was found that a smooth surface is formed since the polymer surface in contact with the glass takes the shape of the glass surface. Smooth surfaces are essential to rule out topographic artifacts on the measurement of mechanical properties.[15,16] The roughness of the surfaces were measured by imaging the surfaces of these polymers with a standard AFM, (Park Scientific Autoprobe) using ultralevers with radii of curvature of the order of 20 nm. The rms roughness is around 20 nm on a 60 μm × 60 μm scale. On areas 200 nm × 200 nm, the rms roughness on this scale is <1 nm. The chemistry of the surface was analyzed by X-ray photoelectron spectroscopy (XPS)[17] with a Perkin-Elmer ESCA 5000 series instrument. XPS is a surface sensitive technique (probing depth) providing chemical information in the form of core level electronic excitation peaks characteristic of the chemical environment of the surface. A carbon and oxygen peak was seen. The amount of oxygen on the surface is small (<5%). The oxygen is there because the sample was heated in air. However no other contaminant like Si or Na from the glass was observed. The contact angle of methylene iodide and water was measured on the polymer surfaces using a Rame-Hart contact angle goniometer, and was found to be approximately 95 and 52°, respectively on all the polymers. These values are in agreement with literature values for the polymers.[13,18−20].

Table 1. Polymers Used in the Experiments and Their Properties[a]

polymer	properties of the original polymer obtained from the supplier	% crystallinity after molding
low density polyethylene (LDPE)	density = 0.92 g/cm^3 T_m = 115 °C	~23
high density polyethylene (HDPE)	$M_w = 125 \times 10^3$, T_m = 131 °C density = 0.95 g/cm^3	~65
isotactic polypropylene (IPP)	$M_w = 250 \times 10^3$ T_m = 189 °C, T_g = −26 °C density = 0.90 g/cm^3	~63
atactic polypropylene (APP)	viscosity = 23 poise T_g = −10 °C	<2

[a] The percent crystallinity was obtained by measuring heats of fusion of the final sample, i.e. after molding, by DSC in our laboratory.

The properties of the polymers are listed in Table 1. The percentage crystallinity of the processed film was determined by measuring heats of fusion by differential scanning calorimetry (DSC)[21] on a Perkin-Elmer (DSC 7) differential scanning calorimeter. The heats of fusion were determined by integrating the peaks obtained on the resulting polymers at the melting point. The ratio of the heat of fusion measured to the heat of fusion of a 100% crystalline sample gives an approximate measure of the percent crystallinity of the sample. The heats of fusion for 100% crystalline polyethylene and polypropylene used were 295.8 and 208.8 J/g, respectively.[22] HDPE and IPP are highly crystalline materials as opposed to LDPE and APP. This is expected, and the effect of density and tacticity on the degree of crystallinity has been discussed in detail elsewhere.[23]

The Instrument. The continuum force microscope (CFM) used to measure the mechanical properties uses fiber optic interferometry to measure the motion of the cantilever.[24] A fiber optic is impinged on the back of the cantilever. This forms an interference cavity, as light reflected back from the edge of the fiber optic and that reflected off the back of the cantilever interfere. This interference pattern is a periodic function of the wavelength of the light used (in our case 780 nm), and hence movement of the tip is calibrated against the wavelength of light used and is very accurate. The normal and lateral forces are measured independently by two separate fiber optic cables; hence, the signals measured for the vertical and horizontal displacement of the cantilever are independent of each other. The cantilever is prepared by bending a tungsten wire at a right angle and etching the end to a sharp tip. The resonance frequency of the cantilever was measured by oscillating it at different frequencies and was found to be 16 kHz. The diameter of the cantilever was measured with a micrometer. The force constant was then calculated from the resonance frequency, diameter, and the density and elastic modulus of bulk tungsten. The cantilever was approximated as a cylinder of circular cross section, clamped at one end and free at the other. We can back-calculate the length of the cantilever from the above treatment and measure the length independently to check for any discrepancies. The force constant of the tip is 235 N/m (±15%). The primary error comes from the measurement of the diameter; this is because the force constant of the tip scales as the diameter to the fourth

power. To better understand the mechanical properties, the radius of the tip was measured by imaging the stepped surface, (305) of strontium titanate[25] in the contact mode. The ridges on this surface are sharper than the tip, and hence the image obtained reflects the tip profile. The radius was determined by fitting a parabola to the features scanned and extracting a radius of curvature of 1000 nm.[26] In all experiments, the sample is scanned using a piezoelectric tube with respect to the tip. All measurements were done while purging the chamber with dry nitrogen to avoid capillary condensation of water at the contact between the tip and the surface.[27,28] Humidity levels are below 10% when this is done.

Elastic Modulus. To measure the elastic modulus of the sample the tip was oscillated at a frequency (1.5 kHz) far below its resonance frequency (16 kHz) with an amplitude of 1−1.5 nm. This was done by applying an ac signal to a piezoelectric chip on which the tip was mounted. This amplitude was then measured by lock-in techniques.

Hardness. Hardness was measured by indentation and was defined as the load divided by the projected area of the indent after the load was removed. Typical loads used were 5−50 μN. Typical diameters of the indents were on the order of 1 μm.

Friction. Friction was measured by scanning a line around 200 nm in length. The scan speed was around 10^{-6} m/s. After each line scan, the load is increased by ramping the voltage applied to the scan piezoelectric tube. The force constant for the lateral displacement of the cantilever was assumed to be the same as that for the vertical displacement. The difference in frictional force between left and right scans gives us twice the frictional force.[29] This is done because it is difficult to establish the zero of the frictional force.

Theory used in the evaluation of elastic modulus. The experimental set up is similar to that used in phase imaging and forced oscillation AFM.[30−32] In the present experiment we modulate the tip, instead of the sample. Since we wish to quantitatively analyze the elastic modulus dependence on load, a brief theoretical description of our experimental setup is detailed below. The experiment can be modeled as follows. The tip is treated as a forced oscillator with damping.[33,34] In the experiments the phase of the lock-in amplifier is set to maximize the output signal A of the lock-in amplifier, far away from the surface. It has been shown by Salmeron et al.[34] that the expression for the in-phase component of the oscillation when this is done is

$$A = \frac{aQ}{(1 - \delta + \delta^2 Q^2)^{1/2}} \frac{1 - \delta + \delta(\delta - f'(z))Q^2}{1 - \delta + (\delta - f'(z))^2 Q^2} \qquad (2)$$

Here a is the amplitude of the applied oscillation of the tip out of contact, $\delta = 1 - \omega^2/\omega_0^2$ where ω is the frequency at which the tip is driven and ω_0 is the resonance frequency of the tip. Q is the quality factor of the cantilever and is related to the frictional forces acting on the tip or the width of the resonance peak. $f'(z)$ is the derivative of the interaction force between the tip and the surface in units of the force constant of the tip, defined as

$$f'(z) = \frac{1}{k}\frac{dF}{dz} \qquad (3)$$

Let us call the derivative of the interaction force with distance as the stiffness of the junction (S), so that $S = dF/dz$.

We measure A, at a frequency $\omega^2 \ll \omega_0^2$, so that $\delta = 1$. Then eq 2, for repulsive loads, becomes

$$A \approx \frac{a}{1 - f'(z)} = \frac{ak}{S + k} \qquad (4)$$

Thus since $S = k(a/A - 1)$ if we measure A, we have determined S. This expression is the same as that obtained by Pethica et al.[11,35]

Now let us examine the quantity S. In noncontact, S is related to the attractive van der Waals potential[36] but is very difficult to model quantitatively as the tip is in contact with the surface for only a fraction of its period of oscillation. To get the elastic modulus of the sample, we analyze S, where the tip is always in contact with the sample. Thus the amplitude of oscillation must be smaller than the mean deflection (load) of the tip, i.e.

$$a \le \frac{W}{k} \qquad (5)$$

In the present experiment this occurs only at loads above ∼300 nN. At loads above ∼300 nN we can apply Hertzian contact mechanics[12] (the Hertz contact describes a purely elastic contact between a sphere of radius R and a planar surface) which gives us

$$S \cong 1.8 E^{*2/3} W^{1/3} R^{1/3} \qquad (6)$$

where W is the external load applied, R is the radius of the tip, and E^* is the modified elastic modulus of the junction defined as

$$\frac{1}{E^*} = \frac{1 - \nu_1^2}{E_1} + \frac{1 - \nu_2^2}{E_2} \qquad (7)$$

where E_1 and E_2 are the elastic modulus of the polymer and tip respectively and ν_1 and ν_2 are the Poisson ratios of the polymer and tip, respectively. (When a material is stretched in one direction it contracts in a direction at right angles to the direction of stretching, this ratio is the Poisson ratio of the material. It is always a positive number less than 0.5.)[33]

If we assume the tip to be composed of tungsten or tungsten oxide then $E_1 \ll E_2$. Thus we can approximate the above equation as

$$\frac{1}{E^*} \approx \frac{1 - \nu_1^2}{E_1} = \frac{1}{E_1^*} \qquad (8)$$

Thus if we measure A at a fixed load W with a tip of radius of curvature R, we can determine E_1^*. Since all the above polymers have Poisson ratios in a similar range,[37] we are mainly measuring differences in E_1, the elastic modulus of the polymer. Also it should be noted from eq 6 that the effect of an error in the measurement of R does not have a very pronounced effect on the value of E^*. Another important point is that for a tip radius 1000 nm, S is in the range 15−250 N/m for the polymers examined for loads ranging from 1 to 100 nN; hence, it is important to choose a tip with a large force constant k, so that the damping (A/a) is not too significant and can be measured with a good signal-to-noise ratio.

Results and Discussion

Stiffness. Shown in Figure 2 are plots of load W and amplitude damping (A/a) in percentage vs sample displacement, obtained simultaneously on IPP, while approaching and retracting the sample and the tip. Initially the tip is out of contact and the load and amplitude damping are unchanged. As the tip approaches the surface, the amplitude gets damped. There is further damping in repulsive contact of the tip and the surface, depicted by an increase in the load and a decrease in the amplitude. When the tip is retracted, a similar behavior is observed; there is, however, some hysteresis. This hysteresis is related to pull-off forces, piezo hysteresis, and inelastic forces and is difficult to quantify.

From approach curves such as those in Figure 2 we have obtained values for the elastic modulus from eqs 4, 6, and 8. We have assumed Poisson ratios (ν_1) of 0.34 for polyethylene and 0.32 for polypropylene[37] in the calculation. We have then plotted, in Figure 3, the

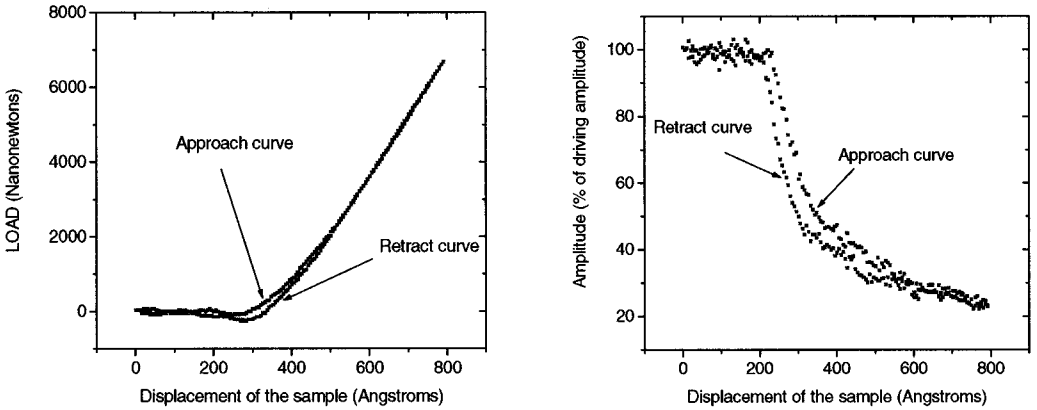

Figure 2. (a) Plot of vertical displacement of the cantilever of load (W) vs sample displacement. (b) Plot of the amplitude damping (A/a) vs sample displacement. Both the curves were obtained simultaneously on IPP.

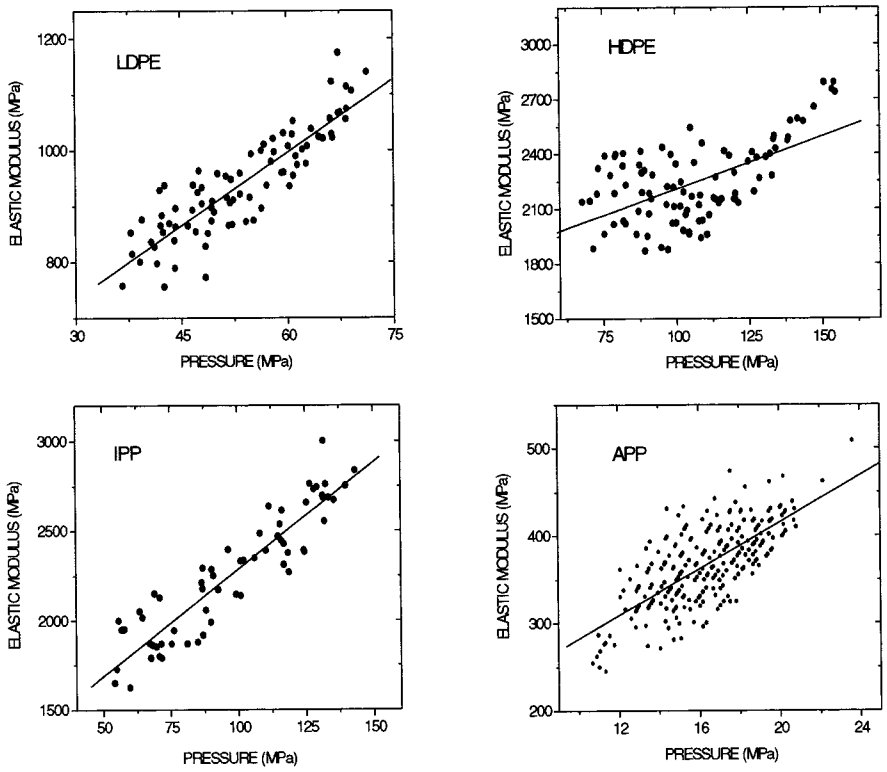

Figure 3. Plot of the elastic modulus E, measured on LDPE, HDPE, IPP, and APP vs mean contact pressure P (defined by eq 1). The lines drawn represent linear fits to the data as expected by eq 9. We have obtained values for E_0 and β, which are listed in Table 2.

elastic modulus vs mean contact pressure (given by eq 1) on sample approach, for loads when contact is maintained during the entire period of oscillation of the tip (i.e., the condition in eq 5), i.e., above loads of ~300 nN. Although the load regime analyzed (~300−5000 nN) is similar for all the polymers, the contact pressure depends on the elastic modulus of the polymer and hence is different for different polymers.

In this repulsive load regime, the Hertzian theory is a good approximation to study the effect of increasing load or pressure on the elastic modulus. The elastic modulus is seen to increase with mean contact pressure for all the polymers studied. To explain this we note that, in the contact region, a large component of the pressure under the tip is hydrostatic. It is known that the elastic moduli of these polyolefins increases with hydrostatic pressure.[37−40] The increase in elastic modulus of the polymer with increasing pressure has been attributed to two effects:

(a) an increase in the density of the polymer, which increases the interactions among polymer chains, thereby increasing the elastic modulus;[40]

(b) changes in the relaxation dynamics of polymer chains which increase the elastic modulus.[38] The amorphous or disordered component of the polymer is more sensitive to these changes.

We find the relation of elastic modulus, (E) vs mean contact pressure (P) to agree with the expression observed in high-pressure experiments,[37−38] of the form

$$E = E_0 + \beta P \tag{9}$$

We have fit expressions of this form to the data and have obtained values for the extrapolated elastic modulus at zero pressure, (E_0) and the constant of proportionality (β). These values are listed in Table 2. The constant β decreases with increasing density of the polymer. This is reasonable, since the effect of high

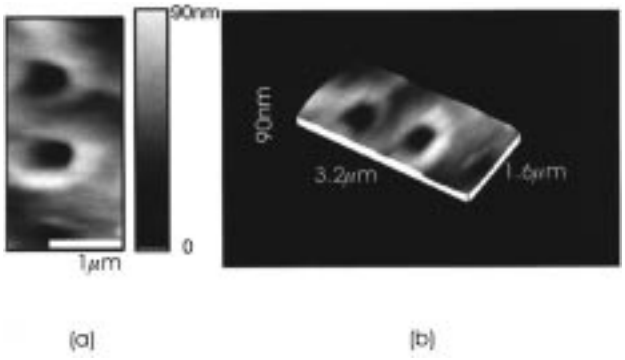

Figure 4. Topographic image of the indents formed on HDPE, after indenting with loads of 29 and 34 μN. Microhardness values were obtained from such indents and are listed in Table 2.

Table 2. Average Values of the Extrapolated Elastic Modulus E_0, the Constant β (Obtained from Line Fits in Figure 3), and Hardness Values (±25%) Measured on the Polymers

polymer	E_0 (GPa)	β	hardness (MPa)
LDPE	0.47	8.8	22
HDPE	1.6	5.7	60
IPP	1.09	11.9	125
APP	0.15	13.3	1.4

pressure is to increase the density of the polymer,[40] and thus a larger pressure effect is seen on a low-density polymer such as LDPE or IPP than on an already densely packed HDPE. The values of E_0 obtained from the curves fall into the range of elastic moduli expected on the polymers.[41,42] The expected trend of increasing elastic moduli with increasing density and crystallinity is observed. It is known that HDPE has a higher elastic modulus than LDPE due to an increase in density, and this is what we see. For the polypropylenes, an isotactic sample allows good packing of the chains which increases crystallinity substantially; this explains the higher values of elastic modulus of IPP as compared to APP.

Hardness. The hardness values obtained by microindentation, and defined as the load divided by the projected area of the indent are tabulated in Table 2. There is a considerable error bar on the hardness measurements; this is because the indent is not uniform, and it is thus difficult to measure the area accurately. Moreover tip effects are observed, i.e., the fact that we are imaging the indent with the same tip that was used for indentation results in imaging artifacts. The expected trend of increasing hardness with increasing crystallinity is observed, and we can comment qualitatively on the relative yield strengths of the polymers. The hardness values compare well with literature values obtained by Vickers indentation,[43,44] and no pressure effects could be observed.

Friction. In Figures 5 and 6 we have plotted the frictional force vs load for the various polymers. The standard deviation is around 50 nN. Since we have measured friction on all the polyolefins at the same speed and the same temperature, we do not expect the viscoelastic properties of the polymers to play a major role in determining the relative behavior of these very similar polyolefins.

Any reasonable model for friction includes to first order four quantities: (1) the adhesion of the interface being sheared; (2) the yield strength of the material; (3) the elastic modulus of the material; (4) the shear strength of the material.

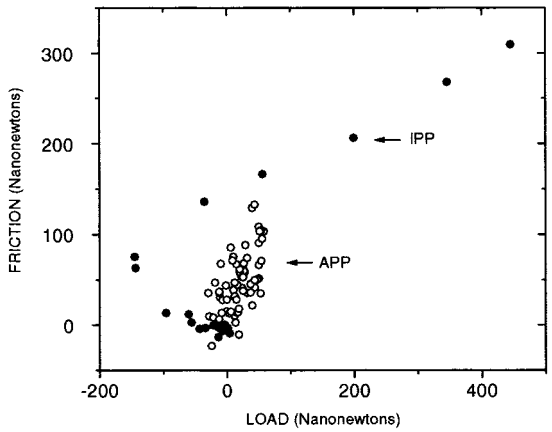

Figure 5. Effect of yield strength of the polymer in determining frictional behavior. Atactic polypropylene (APP) is amorphous, which results in a very low yield strength. The friction is dominated by wear of the sample even at low loads which results in jumps in the frictional force and a very steep slope or friction coefficient as compared to the crystalline isotactic polypropylene (IPP).

For LDPE, HDPE, IPP, and APP it is known in the literature,[13,18−20] and also from our own contact angle measurements that the critical surface tensions, indicative of the surface energy or adhesion of the interface are similar. This is because these polyolefins are all composed of similar hydrophobic monomeric units of carbon and hydrogen only. Thus we do not expect *adhesion* or *surface energy* of the interface to influence the relative frictional behavior of LDPE, HDPE, and IPP significantly.

The importance of the *yield strength* of the polymer in determining friction is seen by comparing friction vs load curves for the chemically similar polypropylenes APP and IPP (Figure 5). APP is amorphous, which results in a very low yield strength, as compared to IPP as can be seen in the low hardness value of APP as compared to IPP. We see a lot of jumps in the frictional force on APP; this is due to the fact that there is considerable wear of this sample even in the low load regime. A very high friction coefficient 0.75 is observed, and this is due to wear of the sample. For IPP, however, we get uniform friction data and a much lower friction coefficient around 0.3. Because of sample wear it was not possible to measure the friction on APP reproducibly at high loads.

LDPE, HDPE, and IPP have significantly higher yield strengths than APP (see hardness values). We could not resolve any wear of LDPE, HDPE, and IPP in the range of loads over which friction was measured. It is true that we are using a tip with a large radius of curvature and are unable to resolve nanoscopic wear; however, our friction data show no jumps and are reproducible. Hence, to a first approximation, we are measuring frictional properties of these polyolefins in the *elastic regime* and the effect of *yield strength* on the frictional behavior of these polyolefins can be neglected. The *elastic modulus* and *shear strength* of LDPE, HDPE, and IPP (or polymer deformation) control their relative frictional behavior in the load regime investigated (0−2 μN).

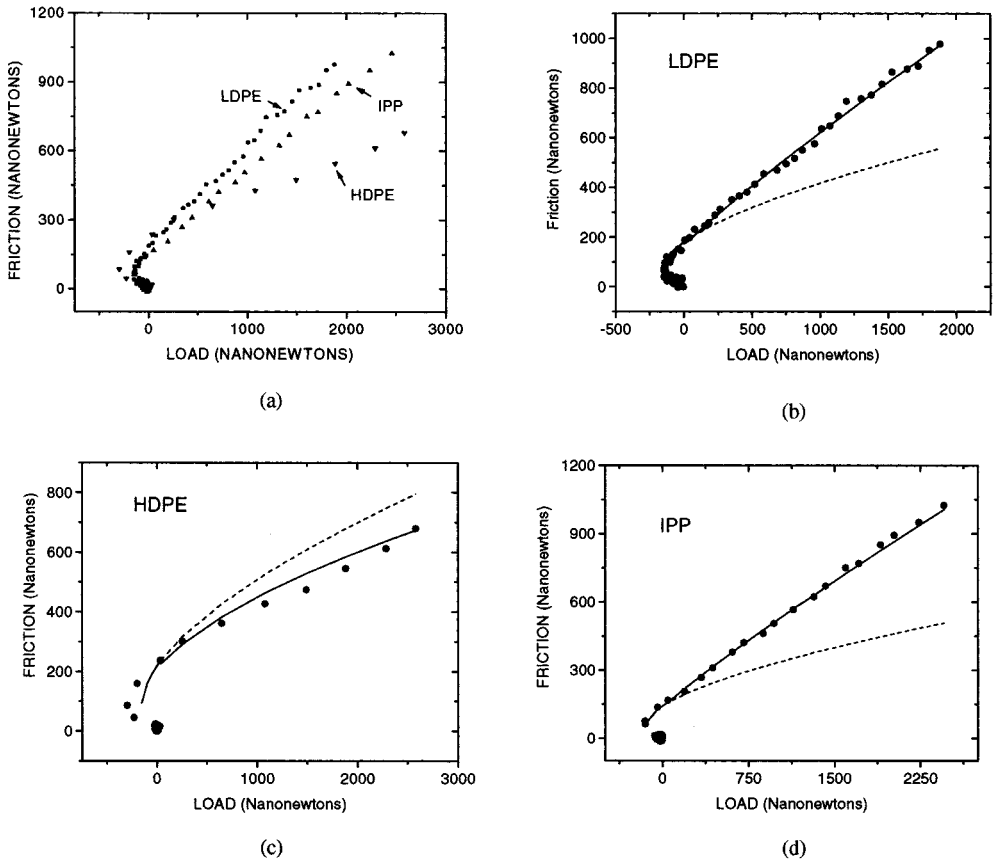

Figure 6. (a) Scatter graphs representing plots of friction (F) vs load (W) measured experimentally on LDPE, HDPE, and IPP. In parts (b), (c), and (d), the dashed line represents curve fits to the friction data as expected by eq 13 for LDPE, HDPE, and IPP, respectively. As can be seen from the poor fit, eq 13 must be modified in the repulsive load regime to include the effects of high pressure under the AFM tip. The solid lines are theoretical curve fits to the data as expected by eq 17 (which includes the high-pressure effects). From these curves estimates of the shear strengths of the polymer were obtained and listed in Table 3.

In the elastic regime, all models for friction assume that the frictional force is

$$F = \tau A \tag{10}$$

where τ is the shear strength of the material and A is the contact area.

There are many models which describe elastic contact of a single asperity (i.e., the tip) with a planar surface; we will invoke the JKR model.[14,45] This we do because we see friction at negative loads that is predicted by the JKR model. Also we do get pull-off forces, i.e., a finite force required to separate the tip and the surface, but they are not sharp (this is due to the large force constant or stiffness of the AFM tip). Moreover, experiments done with the surface force apparatus (SFA) on polymers are in good agreement with the JKR model.[45] Note that the contact pressure is considerably lower in the SFA where smooth surfaces are in contact with each other over large areas..

The JKR model expresses the contact area A between a single asperity and a surface as

$$A = \left[\frac{3\pi^{3/2}R}{4E^*}[W + 3\pi R\gamma + \sqrt{6\pi R\gamma W + (3\pi R\gamma)^2}]\right]^{2/3} \tag{11}$$

where E^* is the modified elastic modulus of the junction as defined above, γ is the surface energy per unit area (i.e. the work per unit area required to separate the surfaces from contact to infinity), R is the radius of curvature of the tip, and W is the load applied.

The JKR model suggests a finite contact area A_0 at zero load, which is given by

$$A_0 = \pi\left(\frac{9\pi\gamma R^2}{2E^*}\right)^{2/3} \tag{12}$$

The JKR model gives an expression for contact area, in our experiments we do not measure contact area but frictional force (F) which is a product of the contact area (A) and shear strength (τ). From eqs 10 and 11, this is given by

$$A = \left[\frac{3\pi^{3/2}R}{4E^*}[W + 3\pi R\gamma + \sqrt{6\pi R\gamma W + (3\pi R\gamma)^2}]\right]^{2/3} \tag{13}$$

In Figure 6 we have plotted the friction (F) vs load (W) measured (in the elastic regime) on LDPE, HDPE, and IPP. We have tried to fit eq 13 to the friction curves obtained experimentally; the curve fits are depicted by the dashed lines in Figure 6. It can be seen from the figure that the frictional force *does not* exhibit the functional dependence on load as expected by eq 13 in the repulsive load regime. This does not mean that the JKR model is inapplicable; instead, the experimental data can be explained by noting that the shear strength of the polymer, τ, is not a constant, but increases linearly with pressure P. Many authors[19,39,46] have suggested an expression of the form

$$\tau = \tau_0 + \alpha P \tag{14}$$

Table 3. Values for τ_0, the Shear Strength of the Polymer at Zero Load, and α for LDPE, HDPE, and IPP[a]

	τ_0 (MPa)		α	
polymer	expt	lit.	expt	lit.
IPP	9	5[19]	0.24	0.17[19]
HDPE	17	14−28[48] 2.5−14[19]	∼0	(0.03−0.09)[48]
LDPE	6	6[19]	0.3	0.14[19]

[a] These values were obtained by fitting eq 17 to the experimental friction vs load curves. The fitting parameter $\gamma = 32$ mJ/m^2 was used for all the polymers. (This was a typical value seen from approach curves such as those in Figure 2.) The parameters used for the functional dependence of elastic modulus on pressure are those measured and listed in Table 2. Literature values for τ_0 and α vary widely depending on strain rate and the type of experiment, and it is difficult to compare numbers exactly, however the numbers obtained from the fit are of the right order of magnitude.

Thus the expression for frictional force in eq 13 must be modified in the repulsive load regime, to take into account the dependence of shear strength on the load or pressure (eq 14). The modified expression for friction in this region is

$$F = (\tau_0 + \alpha P)A = \tau_0\left[\frac{3\pi^{3/2}R}{4E^*}(W + 3\pi R\gamma + \sqrt{6\pi R\gamma W + (3\pi R\gamma)^2})\right]^{2/3} + \alpha W \quad (15)$$

(Note: $PA = W$; e.g., the pressure multiplied by the contact area is the load and hence the second term that has a linear dependence on load.)

And the frictional force at zero load is

$$F_0 = \pi\tau_0\left(\frac{9\pi\gamma R^2}{2E^*}\right)^{2/3} \quad (16)$$

This introduces another variable α, which is the pressure coefficient of the shear strength. This quantity is small and only becomes significant at high pressures, which is what we have under the AFM tip. The effect of α is to introduce a linear behavior of the friction force vs load in this high-pressure regime where the second term in eq 15 becomes significant. The elastic modulus E^* (in eq 15) also depends on pressure or load as measured above and a functional dependence of elastic modulus on load (eqs 1 and 9) must be introduced in eq 15 for an exact expression.

Thus the exact equation for friction (introducing the increase of elastic modulus with load), after taking into account pressure effects on the measurement, is

$$F = \tau_0\left[\frac{3\pi^{3/2}R}{4(E_0^* + \text{const}^* W^{1/3})}(W + 3\pi R\gamma + \sqrt{6\pi R\gamma W + (3\pi R\gamma)^2})\right]^{2/3} + \alpha W \quad (17)$$

We have measured the dependence of elastic modulus on pressure; hence, the unknowns in eq 17 are the shear strength at zero load τ_0 and the pressure coefficient of the shear strength α_0.

Equation 17 fits the experimental data very well, and we have obtained estimates for τ_0 and α. These values are listed in Table 3 along with literature values for the same. The values seem to be of the right order of magnitude. Although there have been attempts to interpret the significance of τ_0 and α in microscopic terms using Eyring theory, these parameters are best regarded as empirical constants.[46] The effects of high pressure on the shear strength of LDPE and IPP are similar. We could not observe any significant pressure effect on the shear strength of HDPE. To explain this, we note that the density of both LDPE and IPP are lower than that of HDPE. The increase in density with increasing pressure follows the trend LDPE > IPP > HDPE;[47] i.e., for the same increase in pressure, the increase in density is the smallest for HDPE (because it is already a dense well-packed polymer). This could be a reason the value of α is the smallest for HDPE. However an exact interpretation of τ_0 and α requires a more detailed theoretical analysis and is not the focus of this paper. The small pressure effect of the shear strength in HDPE explains the low friction coefficient observed on the polymer.

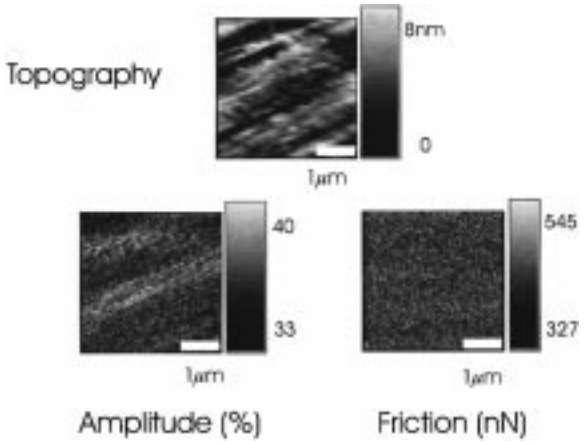

Figure 7. Maps of topography, amplitude damping (A/a), and friction obtained simultaneously on IPP at a load of 800nN. The maps are uniform; i.e., no significant spatial variations of the quantities are observed. This implies that the tip is averaging over crystalline and amorphous domains, and nanoscale spatial variation of these quantities is not possible with the CFM

Spatial variation of Elastic Modulus and Friction. In addition to measuring the elastic modulus and friction as a function of increasing load, we have spatially mapped out these quantities on the polymer surfaces. We obtained uniform maps (Figure 7), and no significant spatial variation of these quantities is observed. This is because of the large radius of curvature of the CFM tip and hence the large contact area, which is larger than the characteristic size of the crystalline and amorphous domains. This results in an average value for these quantities over the domains. This is a limitation of the CFM, and we would have to use sharper tips or AFM to map out these quantities with nanoscale spatial resolution (at higher contact pressures), which has been successfully carried out in various other studies.[30−32]

Conclusions. We have demonstrated that the pressure applied to polymers is an important factor in determining the mechanical response of the polymer; the effect of pressure in any similar measurements with the AFM or CFM cannot be neglected.

In macroscopic real friction between two solids, contact occurs only at very few microscopic junctions, where the pressure is very high. Thus the effects of high pressure in friction experiments are crucial in explaining the friction observed in real systems, and the low-pressure response of the shear strength is responsible for the low friction observed on HDPE.

Acknowledgment. This work was supported by the Director, Office of Energy Research, Office of Basic Energy Sciences, Materials Sciences Division, of the U.S. Department of Energy under contract number DE-AC0376SF00098.

References and Notes

(1) Binnig, G.; Quate, C. F.; Gerber, Ch. *Phys. Rev. Lett.* **1986**, *56*, 9, 930−933.
(2) Bowden, F. P.; Tabor, D. *The Friction and Lubrication of Solids II;* Oxford University Press: London, 1964; pp 214−241.
(3) Bely, V. A.; Sviridenok, A. I.; Petrokovets, M. I.; Savkin, V. G. *Friction and Wear in Polymer-Based Materials*; Pergammon Press Ltd.: New York, 1982.
(4) Bartenev, G. M.; Lavrentev, V. V. *Friction and Wear of Polymers*; Elsevier Scientific: New York, 1981.
(5) Briscoe, B. J. In *Adhesion 5*; Allen, K. W., Ed.; Applied Science Publishers Ltd.: London, 1981; Chapter 4, pp 49−81.
(6) Ward, I. M. *Mechanical Properties of Solid Polymers*, 2nd ed.; Wiley: New York, 1983.
(7) Overney, R.; Meyer, E. *MRS Bull.* **1993**, *18*, 5, 26−34.
(8) Aime, J. P.; Eikaakour, Z.; Odin, C.; Bouhacina, T.; Michel, D.; Curely, J.; Dautant, A. *J. Appl. Phys* **1994**, *76*, 1754−1762.
(9) Heuberger, M.; Dietler G.; Schlapbach, L. *Nanotechnology* **1994**, *5*, 12−23.
(10) Mate, C. M. *IBM J. Res. Dev.* **1995**, *39*, 6, 617−627.
(11) O'Shea, S. J.; Welland, M. E.; Pethica, J. B. *Chem. Phys. Lett.* **1994**, *223*, 336−340.
(12) Johnson, K.L *Contact Mechanics*, 1st ed.; Cambridge University Press: New York, 1987; pp 84−105.
(13) Pooley, C. M.; Tabor, D. *Proc. R. Soc. London, A* **1972**, *329*, 251−274.
(14) Johnson, L.; Kendall, K.; Roberts, A. D. *Proc. R. Soc. London, A* **1971**, *324*, 301−313.
(15) Mizes, H. A.; Loh, K. G.; Miller, R. J. D.; Ahuja, S. K.; Grabowski, E. F. *Appl. Phys. Lett.* **1991**, *59*, 22, 2901−2903.
(16) Barrett, T. S.; Stachowiak, G. W.; Batchelor, A. W. *Wear* **1992**, *153*, 331−350.
(17) Woodruff, D. P.; Delchar, T. A. *Modern Techniques of Surface Science*, 1st ed.; Cambridge University Press: New York, 1989; p 96.
(18) Fox, H. W.; Zisman, W. A. *J. Colloid Sci.* **1952**, *7*, 428−442.
(19) Briscoe, B. J.; Tabor, D. *J. Adhes.* **1978**, *9*, 145−155.
(20) Wu, S. *Polymer Interface and Adhesion*; Marcel Dekker: New York, 1982; p 184.
(21) Billmeyer, F. W. *Textbook of Polymer Science*, 3rd ed.; Wiley-Interscience: New York, 1984; p 242.
(22) Mandelkern L.; Alamo R. G. In *Physical Properties of Polymer Handbook*; Mark, J. E., Ed.; American Institute of Physics: New York, 1996; p 123.
(23) Cowie, J. M. G. *Polymers: Chemistry and Physics of Modern Materials*; Intext Educational Publishers: New York, 1973; Chapter 10.
(24) Rugar, D.; Mamin, H. J.; Guethner, P. *Appl. Phys. Lett.* **1989**, *55*, 2588−2590.
(25) Sheiko, S.; Moller, M.; Reuvekamp, E. M.; Zandbergen, H. W. *Phys. Rev. B* **1993**, *48*, 5675−5678.
(26) Carpick, R. W.; Agrait, N.; Ogletree, D. F.; Salmeron, M. *J. Vac. Sci. Technol. B* **1996**, *14*, 2, 1289−1295.
(27) Somorjai, G. A. *Introduction to Surface Chemistry and Catalysis*; Wiley-Interscience: New York, 1994; p 294.
(28) Fogden, A.; White, L. *Journal of Colloid and Interface Science* **1990**, *138*, 414−430.
(29) Perry, S. S.; Mate, C. M.; White, R. L.; Somorjai, G. A. *IEEE Trans. Magn.* **1996**, *32*, 115−121.
(30) Kajiyama, T.; Tanaka, K.; Okhi, I.; Ge, S.; Yoon, J.; Takahara, A. *Macromolecules* **1994**, *27*, 7932−7934.
(31) Overney, R. M.; Meyer. E.; Frommer, J.; Guntherodt, H. J.; Fujihara, M.; Takano, H.; Gotoh. Y *Langmuir* **1994**, *10*, 1281−1286.
(32) Chi, L. F.; Anders, M.; Fuchs, H.; Johnston, R; Ringsdorf, H. *Science* **1993**, *259*, 213-216.
(33) Feynman, R. P.; Leighton, R.; Sands, M. *The Feynman lectures on Physics*, Addison-Wesley Publishing Co.: Reading, MA, 1963−65; Vol. 1, Chapter 23, p 3.
(34) Salmeron, M. *MRS Bull.* **1993**, *18*, 5, 20−25.
(35) Pethica, J. B.; Oliver, W. C. *Phys. Scr. T* **1987**, *19A*, 61−66.
(36) Burnham, N. A.; Colton, R. J.; Pollock, H. M. *Nanotechnology* **1993**, *4*, 2, 64−80.
(37) Pae, K. D.; Sauer J. A. In *Engineering Solids under Pressure*; Pugh, H. D., Ed.; The Institution of Mechanical Engineers: London, 1971; pp 69−74.
(38) Radcliffe, S. V. In *Deformation and Fracture of Polymers*; Kausch, H. H., Hassell, J. A., Jaffee, R. I., Eds.; Plenum Press: New York, 1973; p 198.
(39) Towle, L. C. *J. Appl. Phys.* **1973**, *43*, 4, 1611−1615.
(40) Sayre, J.; Swanson, S.; Boyd, R. *J. Polym. Sci., Polym Phys. Ed.* **1978**, *16*, 1739−1759.
(41) Popli, R.; Mandelkern, L. *J. Polym. Sci. Polym. Phys.* **1987**, *25*, 441−483.
(42) Quirk, R. P.; Alsamarraie, M. A. A. In *Polymer Handbook*, 3rd ed.; Bandrup, J., Immergut, H., Eds.; Wiley: New York, 1989; Chapter 5, pp 23, 31.
(43) Salazar, J. M.; Balta Calleja, F. J. *J. Mater. Sci.* **1983**, *18*, 1077−1082.
(44) Lorenzo, V.; Perena, J. M.; Fatou, J. G. *J. Mater. Sci. Lett.* **1989**, *8*, 1455−1457.
(45) Mangipudi, V. S.; Huang, E.; Tirrell, M. *Macromol. Symp.* **1996**, *102*, 131−143.
(46) Briggs, D.; Rance, D. In *Comprehensive Polymer Science*, 1st ed.; Booth, C., Price, C., Eds.; Pergammon Press: New York, 1989; Vol. 2, pp 726−728.
(47) Bogdanov, B. G.; Michailov, M. In *Handbook of Polyolefins* Vasile, C., Seymour, R., Eds.; Marcel Dekker: New York, 1993; p 298−299.
(48) Briscoe, B. J.; Tabor, D. *Wear* **1975**, *34*, 29−38.

MA970683B